Transcranial Two-Photon Imaging of the Living Mouse Brain

Guang Yang, PhD,[1] Feng Pan, PhD,[1] Christopher N. Parkhurst,[1] Jaime Grutzendler, MD,[2] and Wen-Biao Gan, PhD[1]

[1]Molecular Neurobiology Program
Skirball Institute
Department of Physiology and Neuroscience
New York University School of Medicine
New York, New York

[2]Department of Neurology
Yale School of Medicine
New Haven, Connecticut

NOTES

Introduction

The imaging of neurons, glia, and vasculature in the living brain has become an important experimental tool for understanding how the brain works. Transcranial two-photon laser scanning microscopy (TPLSM) imaging of the cortex in living mice is a minimally invasive method that allows repeated imaging of brain cells and vasculature at high optical resolution over intervals ranging from seconds to years (Denk et al., 1990; Grutzendler et al., 2002; Yoder and Kleinfeld, 2002; Stosiek et al., 2003; Theer et al., 2003; Tsai et al., 2004; Davalos et al., 2005; Zhang et al., 2005; Zuo et al., 2005a,b; Haynes et al., 2006; Majewska et al., 2006; Nishiyama et al., 2007; Xu et al., 2007; Kim et al., 2009; Wake et al., 2009; Wu et al., 2009; Yang et al., 2009; Lai et al., 2012). By creating a thinned-skull cranial window with skull thickness ~20 μm, it is possible to image fluorescently labeled structures located up to 300–400 μm within the cortex (Grutzendler et al., 2002; Tsai et al., 2004; Davalos et al., 2005; Zuo et al., 2005a). In recent years, this transcranial imaging approach has been used to study the development and plasticity of synaptic connections (Grutzendler et al., 2002; Tsai et al., 2004; Zuo et al., 2005a,b; Majewska et al., 2006; Nishiyama et al., 2007; Xu et al., 2007; Zhang and Murphy, 2007; Wu et al., 2009; Yang et al., 2009; Lai et al., 2012), neuronal network activity (Stosiek et al., 2003), cerebral vasculature (Yoder and Kleinfeld, 2002), and amyloid plaques (Christie et al., 2001; Tsai et al., 2004; Yan et al., 2009) as well as the structure and function of microglial cells in the living intact cortex (Davalos et al., 2005; Haynes et al., 2006; Wake et al., 2009).

In this chapter, we describe in detail a protocol for imaging cortical structures at high optical resolution through a thinned-skull cranial window in living mice using TPLSM. Surgery can be performed within 30–45 min, and images can be acquired immediately thereafter. The procedure can be repeated multiple times, allowing longitudinal imaging of the cortex over intervals ranging from days to years. Imaging through a thinned-skull cranial window avoids exposure of the meninges and cortex, thereby providing a minimally invasive approach for studying structural and functional changes of cells under normal and pathological conditions in the living brain.

Materials and Methods

Experimental animals

Transgenic mice were used that express fluorescent proteins in the cytoplasm of cortical neurons (e.g., Thy1-YFP [yellow fluorescent protein] line) or CNS resident microglia (e.g., CX3CR1-EGFP [enhanced green fluorescent protein] line) (Feng et al., 2000; Jung et al., 2000). All experiments using animals were carried out under institutional and national guidelines.

Thinned-skull preparation

1. Anesthetize mice by intraperitoneal injection (5–6 μl/g body weight) of 20 mg/ml ketamine and 3 mg/ml xylazine mix (KX). Allow sufficient time (5–10 min) for a surgical level of anesthesia to be achieved. Place the mouse on a cotton pad after a surgical level of anesthesia has been reached. A heating pad may be inserted under the cotton pad in order to maintain a body temperature of ~37°C. Continuously monitor the depth of anesthesia by testing the animal's reflexes (e.g., pinching the animal's foot with a blunt pair of forceps and checking for the absence of the eye-blinking reflex) during the surgery and inject more KX when necessary.

2. Lubricate both eyes with a drop of eye ointment. Thoroughly shave the hair over most of the scalp with a double-edge razor blade. Remove the residual hair and clean the scalp with a sterile alcohol prep pad; then perform a midline scalp incision that extends approximately from the neck region (between the ears) to the frontal portion of the head (between the eyes). Carefully disrupt the fascia located between the scalp and the underlying muscle and skull with a pair of spring scissors, taking care not to sever blood vessels.

3. Localize the brain area to be imaged based on stereotactic coordinates, and mark it with a pen.

4. Remove the connective tissue attached to the skull over the area to be imaged by gently scraping the skull with a blunt microsurgical blade. Local anesthetics may be added to the skull surface to minimize pain associated with drilling of the periostium.

5. Place a small amount of cyanoacrylate glue around the edges of the internal opening of the skull holder, and press the holder against the skull. Skull immobilization, which is in part determined by the quality of the skull holder to skull bonding, is very important for reducing movement artifacts during imaging. Make sure that the area to be imaged is exposed in the center of the internal opening (Fig. 1A).

NOTES

6. Gently pull the loose skin up to the edges of the internal opening of the skull holder, and apply a small amount of glue to the edge of skin to adhere it to the skull. Gluing the skin around the internal opening of the skull holder and the skull helps to hold the artificial cerebrospinal fluid (ACSF) in place during imaging when using a water immersion lens.

7. Wait several minutes until the skull holder is well glued to the skull. Attach the skull holder to the skull immobilization device by gently inserting the lateral edges of the skull holder between the aluminum blocks and washers/screws of the skull immobilization device. Tighten the screws to completely immobilize the skull holder (Fig. 1A). Wash the opening of the skull holder a few times with ACSF to remove remnants of nonpolymerized glue. This helps prevent the glue from contaminating the microscope objectives.

8. Apply a few drops of ACSF to the skull surface during drilling to reduce overheating. Under a dissecting microscope, use a high-speed micro-drill to thin a circular area (typically ~0.5–1 mm in diameter; Fig. 1B) over the skull region of interest. Do not thin a large region (>1.5 mm) to a thin layer (<50 µm) because this would make it difficult to exercise fine control of the drilling process and might cause damage to the underlying cortex. Perform drilling intermittently to avoid friction-induced overheating. Replace the ACSF periodically to wash away the bone debris. The mouse skull consists of two thin layers of compact bone (periosteum and endosteum), sandwiching a thick layer of spongy bone that contains small cavities and canaliculi that carry blood vessels. Remove the external layer of compact bone and most of the spongy bone with the drill. Bleeding may occur during drilling of the spongy bone portion but usually stops spontaneously within a few minutes.

9. After removing the majority of the spongy bone, remaining concentric structures within the bone can usually be seen under the dissecting microscope, indicating that drilling is approaching the internal compact bone layer. At this stage, skull thickness is still greater than 50 µm. At this point, continue the skull-thinning procedure with a microsurgical blade to obtain a very thin (~20 µm) and smooth preparation (~200 µm in diameter) (Fig. 1B). During the thinning process, repeatedly examine the preparation with a conventional fluorescence microscope until the dendrites and spines in the area of interest can be clearly visualized. Hold the microsurgical blade at a ~45° angle during thinning, and take great care not to push the skull downward against the brain surface or to break through the bone, as minor brain trauma or bleeding may induce inflammation and disruption of neuronal structures. The thickness of the skull can be directly measured by imaging the skull autofluorescence with the TPLSM. Periodic measurement of skull thickness during thinning may help to prevent skull overthinning. It is critical not to thin a large surface area

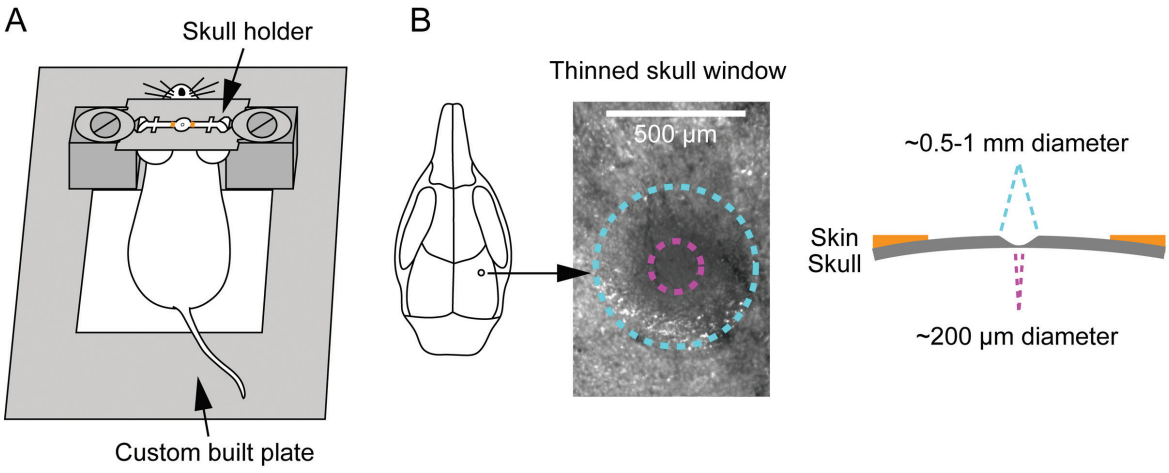

Figure 1. Schematic diagram of thinned-skull preparation. ***A***, A head-immobilization device, including a custom-built plate and a skull holder, is used for reducing movement artifacts during imaging. The skull holder is glued onto the mouse skull and tightened on the aluminum blocks of the custom-built plate. The region of interest is exposed in the center. ***B***, A circular area of skull (typically ~0.5–1 mm in diameter, blue circle) over the region of interest is shaved. The thinnest region (pink circle) for TPLSM imaging is ~20 µm in thickness and ~200 µm in diameter. Scale bar: ***B***, 500 µm.

NOTES

(>300 μm in diameter) to less than 15 μm in thickness because it may disrupt neuronal structures and activate immune cells, as evidenced by neurite blebbing, microglia process retraction, and thickening of epidural connective tissues. These events will reduce the quality of subsequent images and may confound experimental results.

Mapping the imaging area for future relocation

1. In order to identify the same imaged area at a later time point, take a high-quality picture of the brain vasculature with a CCD camera attached either to a stereo-dissecting microscope (Fig. 2A) or directly to the TPLSM setup.

2. Carefully move the prepared mouse with entire skull immobilization device to the TPLSM microscope stage. Select a properly thinned area for imaging under a fluorescence microscope, and carefully mark the selected area on the CCD brain vasculature map by observing the pattern of blood vessels adjacent to it (Fig. 2A). If performing microglial imaging, inject 100 μl of rhodamine-dextran solution retro-orbitally for vessel labeling before applying eye ointment or, alternatively, inject it through the tail vein.

TPLSM imaging of neuronal or glial structures

1. Tune the TPLSM to the appropriate wavelength (e.g., 920 nm for YFP and 890 nm for GFP). When possible, use high numerical aperture water-immersion objectives (e.g., 60×, 1.1 N.A.) to acquire images. The objective lens should remain immersed in mouse ACSF at all times during imaging. If imaging quality suddenly deteriorates, check that the lens remains fully immersed in ACSF, and add more if necessary. Gradual leakage of ACSF is usually caused by inadequate gluing of the scalp around the skull holder openings.

2. For neuronal imaging, obtain a low-magnification stack of fluorescently labeled neuronal processes (e.g., 60× objective; 200 μm × 200 μm; 512 × 512 pixel; 2 μm step), which serves as a higher-resolution map for accurate relocation of the same region at later time points in conjunction with the CCD brain vasculature map (Fig. 2B). If performing microglial imaging, take a low-magnification (10× air objective) stack of the rhodamine-dextran–labeled vasculature and mark the selected area before switching to 40×/60× objective, making sure that the objectives (10× and 40×/60×) are cocentered.

3. Without changing the position of the stage, take high-magnification images (e.g., 66.7 μm × 66.7 μm; 512 × 512 pixel; 0.75 μm step: Fig. 2C) from the same area. The stack is typically taken within ~100 μm below the pial surface for spine imaging and within ~200 μm for microglial imaging. Laser intensities are in the range of 10–30 mW (measured at the sample) to minimize phototoxicity.

Recovery

When imaging is complete, detach the skull holder from the skull by gently pushing the skull away from the skull holder. When removed, the holder should take with it any remaining glue and be separated from the skin. If glue still adheres to the skull or skin, gently remove any remaining dried glue with a pair of forceps. Suture the scalp with 6-0 silk, and leave the mouse in a separate cage until it is fully mobile. After recovery, return the mouse to its original housing cage until the next viewing.

Reimaging

Find the thinned region based on the brain vasculature map (CCD for dendrite imaging, and/or two-photon angiography for microglia). If the second view is within one week after the first view, carefully remove the connective tissue that has regrown on top of the thinned region using a microsurgical blade, and check the image quality with the TPLSM microscope. If the image quality is poor (blurry features, high background fluorescence, or significantly reduced depth of penetration), use a microsurgical blade to carefully shave the skull until a clear image can be obtained. If the second view is more than a week after the first view, a high-speed micro-drill is needed to rethin the region of interest. The bone in the thinned area can regrow substantially if the time interval between imaging sessions is longer than one week. The newly grown bone layer is optically less transparent for TPLSM imaging, so it is generally necessary to shave the bone slightly thinner than in the previous imaging session.

Find the previously imaged region under the fluorescence microscope. Align the region according to the low-magnification map under TPLSM, and then zoom in to high magnification to further align it. After the region is precisely aligned with the first view, take images with TPLSM. Although we have successfully imaged the same region with high optical clarity up to five times, the number and quality of imaging sessions depends upon the quality of the initial surgery, the intrasession interval, and the

NOTES

experience of the operator. While thinning the skull to the extremes (~15 μm) during the first surgery may provide excellent clarity in the initial imaging session, it will make repeated imaging sessions more difficult owing to an increased propensity for compensatory bone regrowth. Therefore, we recommend minimizing the perturbation to the system by limiting the number of imaging sessions and by thinning the skull only as much as necessary to gain an image clear enough to observe the desired structures.

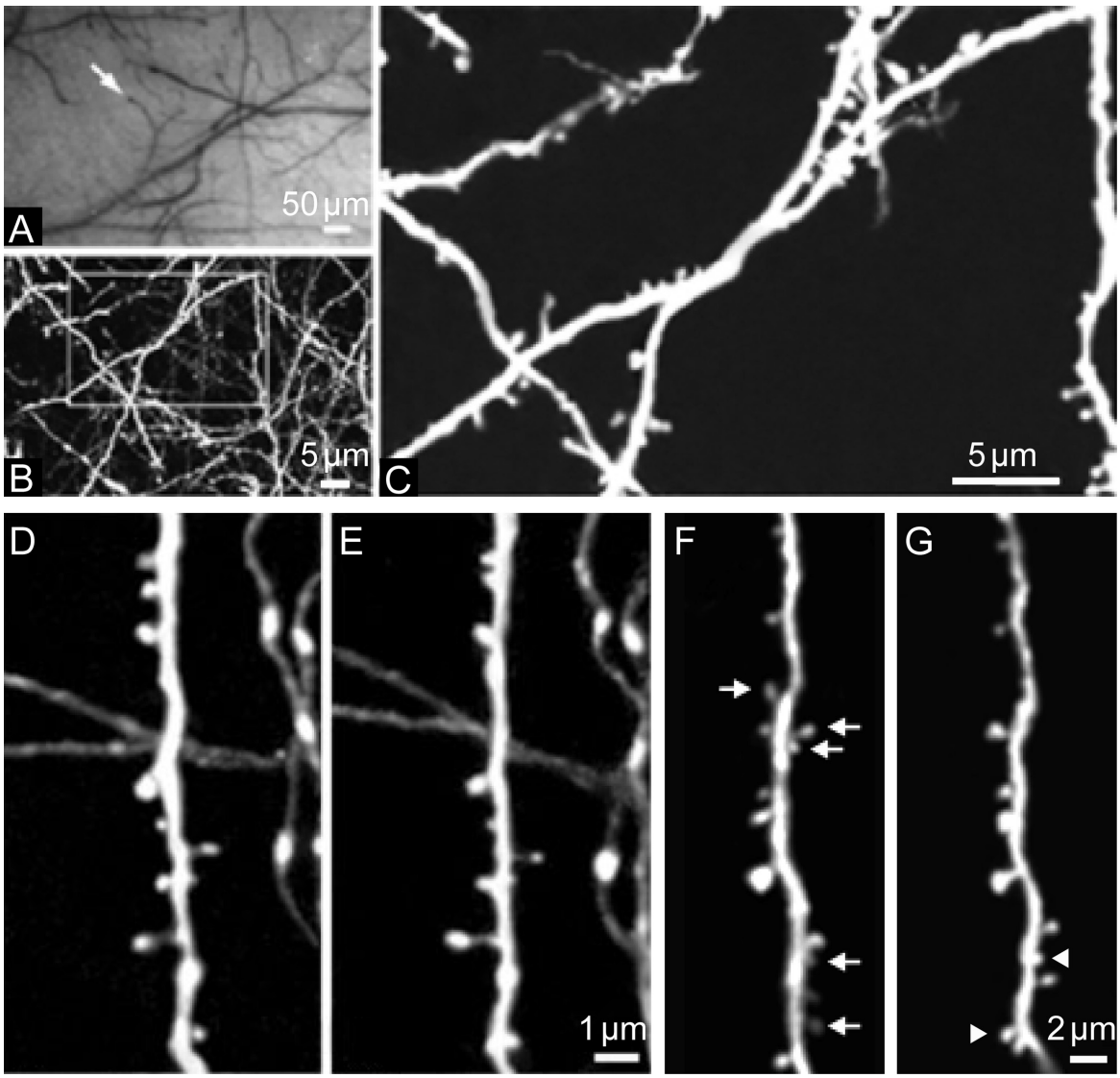

Figure 2. Long-term transcranial TPLSM imaging of fine neuronal structures. ***A***, CCD camera view of brain vasculature under the thinned skull. The cortical vasculature can be clearly seen through the thinned skull. The vasculature pattern remains stable over months to years and can be used as a landmark to relocate the imaged region at subsequent time points. *Arrow:* the region where subsequent TPLSM images were obtained. ***B***, Two-dimensional projection of a 3D stack of dendritic branches and axons in the primary visual cortex (60×, ~0.39 μm per pixel). The stack was 50 μm deep (2 μm step size). The boxed region was then imaged at higher magnification (***C***). High-power 2D projection of a 3D stack (60×, ~0.13 μm per pixel, 10 μm reconstructed, 0.70 μm step size) reveals clear neuronal structures including axonal varicosities, dendritic shafts, and dendritic protrusions. ***D***, ***E***, Axonal and dendritic branches from two animals imaged 3 d apart show the same spines and boutons at the same locations (Grutzendler et al., 2002, their Fig. 3, adapted with permission). ***F***, ***G***, Dendritic branches imaged more than 19 months apart. *Arrows:* spines that are eliminated in the second view. *Arrowheads:* spines that are formed in the second view. Note that most spines in ***F*** persist in ***G*** (Zuo et al., 2005a, their Fig. 4*A* and *B*, adapted with permission). Two-dimensional projections of 3D image stacks containing dendritic segments of interest were used for ***D–G***. Scale bars: ***A***, 50 μm; *B–C*, 5 μm; ***E***, 1 μm; ***G***, 2 μm.

Results

With YFP-expressing mice, this method has been used successfully to image individual dendritic spines and axonal varicosities in various brain areas including visual, somatosensory, motor, and frontal cortices over intervals of up to 19 months (Grutzendler et al., 2002; Zuo et al., 2005a; Yang et al., 2009; Lai et al., 2012). Figure 2*D–E* shows examples of images obtained over a 3 d interval in mice at 4 months of age. Note the remarkable stability of the number and location of adult spines and axonal varicosities between the two views (Fig. 2*D,E*). Most adult spines persist even over a 19-month interval (Fig. 2*F,*G). Because of the noninvasive nature of the thinned-skull technique, this method is also suitable for brain immune-cell imaging (e.g., microglia cells), which are highly sensitive to the environment and respond immediately after perturbation (Davalos et al., 2005; Xu et al., 2007). Figure 3 shows images of GFP-expressing microglial cells in the cortex over days, with minimal changes of their ramified shape under a normal physiological state.

Discussion

Studies in recent years have demonstrated that the transcranial TPLSM imaging approach is minimally invasive and technically reliable, allowing studies of detailed changes of neurons and glia over time in the living intact cortex. The main limitations of the thinned-skull technique are related to the fact that skull thickness is critical for image quality and that the optimal thickness exists within narrow limits. For example, a nonuniform skull thickness may cause significant spherical aberrations, resulting in decreased two-photon excitation and distortion of fluorescent structures located deep in the cortex (Helm et al., 2009). We have found that the skull thickness should ideally be ~20 µm in order to obtain high-resolution images of synapses (Grutzendler et al., 2002; Zuo et al., 2005a; Xu et al., 2007). Conversely, overthinning the skull to less than 15 µm carries the risk of mild cortical trauma resulting from pushing the skull downwards with the drill bit or microsurgical blade. In such cases, the thinning process generally leads to activation of microglia (as manifested by their amoeboid morphology) and is often associated with axonal and dendritic blebbing. Injury of this type can be prevented by carefully using the microsurgical blade at an angle during the thinning procedure and avoiding pushing the skull against the cortical surface. Because of this, consistently achieving an optimal thickness requires significant surgical practice. Furthermore, although multiple imaging sessions within the first few days after initial surgery can be easily performed and require only minimal removal of debris over the thinned cranium, repeated imaging over intervals greater than 2–3 d requires skull rethinning, which may present a challenge for a beginner. Even with

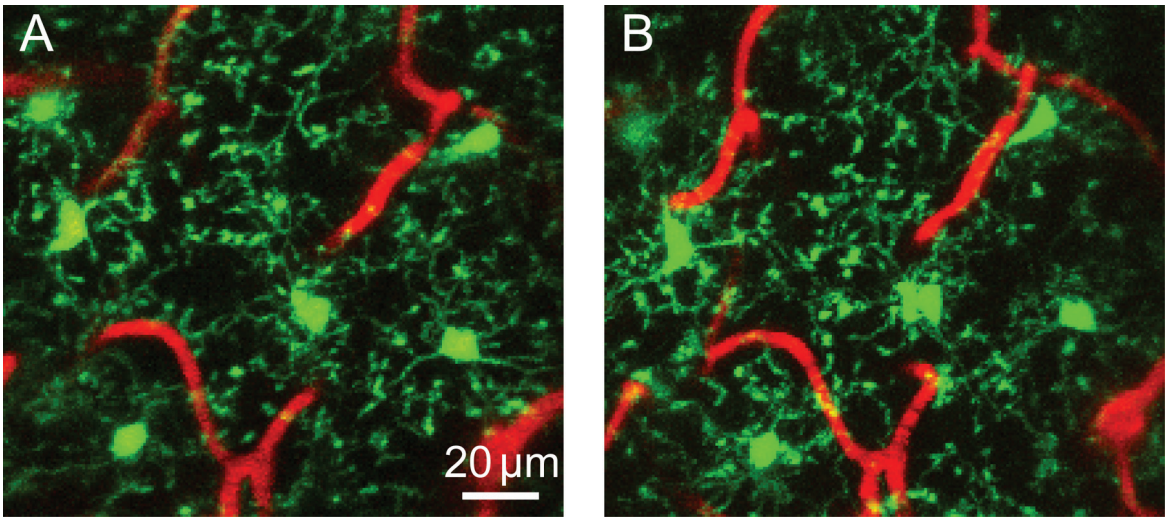

Figure 3. Transcranial TPLSM imaging of EGFP-labeled microglia and cortical vasculature. Two-dimensional projections of a 3D Z-stack from the visual cortex (40×, digital zoom = 1) from a mouse harboring a single copy of the *CX3CR1-EGFP* allele driving EGFP expression in a subset of myeloid cells, including CNS resident parenchymal microglia imaged 24 h apart (***A***, ***B***). The cortical vasculature has been labeled in red by intravenous injection of a rhodamine-dextran conjugate solution. The stacks are 40 µm in depth (1 µm step size) and represent a section of cortex spanning 40–80 µm below the dural surface. EGFP-labeled microglia retain their characteristic highly branched morphology, which indicates a resting state. Scale bar: ***A***, 20 µm.

NOTES

sufficient surgical skill, it is often difficult to perform more than five imaging sessions in the same animal, as the optical properties of the skull may gradually deteriorate with repeated thinning.

TPLSM imaging through a thinned-skull window has emerged in recent years as an important tool for studying structural and functional changes in the living cortex in a minimally invasive manner (Grutzendler et al., 2002; Yoder and Kleinfeld, 2002; Stosiek et al., 2003; Tsai et al., 2004; Davalos et al., 2005; Zhang et al., 2005; Zuo et al., 2005a,b; Haynes et al., 2006; Majewska et al., 2006; Nishiyama et al., 2007; Xu et al., 2007; Kim et al., 2009; Wake et al., 2009; Yang et al., 2009; Lai et al., 2012). With the growing availability of fluorescent reporters to probe the structure and function of the brain (Giepmans et al., 2006; Livet et al., 2007), we envision that transcranial two-photon microscopy (TPM) imaging will greatly expand our understanding of how neural circuits are modified throughout life and how glial and other cells function in the living brain.

Acknowledgments

This paper was published in unabridged format as Thinned-skull cranial window technique for long-term imaging of the cortex in live mice (G. Yang, F. Pan, C.N. Parkhurst, J. Grutzendler, and W.B. Gan) in *Nature Protocols* 2010;5:201–208.

References

Christie RH, Bacskai BJ, Zipfel WR, Williams RM, Kajdasz ST, Webb WW, Hyman BT (2001) Growth arrest of individual senile plaques in a model of Alzheimer's disease observed by *in vivo* multiphoton microscopy. J Neurosci 21:858–864.

Davalos D, Grutzendler J, Yang G, Kim JV, Zuo Y, Jung S, Littman DR, Dustin ML, Gan WB (2005) ATP mediates rapid microglial response to local brain injury *in vivo*. Nat Neurosci 8:752–758.

Denk W, Strickler JH, Webb WW (1990) Two-photon laser scanning fluorescence microscopy. Science 248:73–76.

Feng G, Mellor RH, Bernstein M, Keller-Peck C, Nguyen QT, Wallace M, Nerbonne JM, Lichtman JW, Sanes JR (2000) Imaging neuronal subsets in transgenic mice expressing multiple spectral variants of GFP. Neuron 28:41–51.

Giepmans BN, Adams SR, Ellisman MH, Tsien RY (2006) The fluorescent toolbox for assessing protein location and function. Science 312:217–224.

Grutzendler J, Kasthuri N, Gan WB (2002) Long-term dendritic spine stability in the adult cortex. Nature 420:812–816.

Haynes SE, Hollopeter G, Yang G, Kurpius D, Dailey ME, Gan WB, Julius D (2006) The P2Y12 receptor regulates microglial activation by extracellular nucleotides. Nat Neurosci 9:1512–1519.

Helm PJ, Ottersen OP, Nase G (2009) Analysis of optical properties of the mouse cranium—implications for *in vivo* multi photon laser scanning microscopy. J Neurosci Methods 178:316–322.

Jung S, Aliberti J, Graemmel P, Sunshine MJ, Kreutzberg GW, Sher A, Littman DR (2000) Analysis of fractalkine receptor CX(3)CR1 function by targeted deletion and green fluorescent protein reporter gene insertion. Mol Cell Biol 20:4106–4114.

Kim JV, Kang SS, Dustin ML, McGavern DB (2009) Myelomonocytic cell recruitment causes fatal CNS vascular injury during acute viral meningitis. Nature 457:191–195.

Lai CS, Franke TF, Gan WB (2012) Opposite effects of fear conditioning and extinction on dendritic spine remodelling. Nature 483:87–91.

Livet J, Weissman TA, Kang H, Draft RW, Lu J, Bennis RA, Sanes JR, Lichtman JW (2007) Transgenic strategies for combinatorial expression of fluorescent proteins in the nervous system. Nature 450:56–62.

Majewska AK, Newton JR, Sur M (2006) Remodeling of synaptic structure in sensory cortical areas *in vivo*. J Neurosci 26:3021–3029.

Nishiyama H, Fukaya M, Watanabe M, Linden DJ (2007) Axonal motility and its modulation by activity are branch-type specific in the intact adult cerebellum. Neuron 56:472–487.

Stosiek C, Garaschuk O, Holthoff K, Konnerth A (2003) *In vivo* two-photon calcium imaging of neuronal networks. Proc Natl Acad Sci USA 100:7319–7324.

Theer P, Hasan MT, Denk W (2003) Two-photon imaging to a depth of 1000 μm in living brains by use of a Ti:Al2O3 regenerative amplifier. Opt Lett 28:1022–1024.

Tsai J, Grutzendler J, Duff K, Gan WB (2004) Fibrillar amyloid deposition leads to local synaptic abnormalities and breakage of neuronal branches. Nat Neurosci 7:1181–1183.

Wake H, Moorhouse AJ, Jinno S, Kohsaka S, Nabekura J (2009) Resting microglia directly monitor the functional state of synapses *in vivo* and determine the fate of ischemic terminals. J Neurosci 29:3974–3980.

Wu SH, Arevalo JC, Sarti F, Tessarollo L, Gan WB, Chao MV (2009) Ankyrin Repeat-rich Membrane Spanning/Kidins220 protein regulates dendritic branching and spine stability *in vivo*. Dev Neurobiol 69:547–557.

Xu HT, Pan F, Yang G, Gan WB (2007) Choice of cranial window type for *in vivo* imaging affects dendritic spine turnover in the cortex. Nat Neurosci 10:549–551.

Yan P, Bero AW, Cirrito JR, Xiao Q, Hu X, Wang Y, Gonzales E, Holtzman DM, Lee JM (2009) Characterizing the appearance and growth of amyloid plaques in APP/PS1 mice. J Neurosci 29:10706–10714.

Yang G, Pan F, Gan WB (2009) Stably maintained dendritic spines are associated with lifelong memories. Nature 462:920–924.

Yang G, Pan F, Parkhurst CN, Grutzendler J, Gan WB (2010) Thinned-skull cranial window technique for long-term imaging of the cortex in live mice. Nat Protoc 5:201–208.

Yoder EJ, Kleinfeld D (2002) Cortical imaging through the intact mouse skull using two-photon excitation laser scanning microscopy. Microsc Res Tech 56:304–305.

Zhang S, Murphy TH (2007) Imaging the impact of cortical microcirculation on synaptic structure and sensory-evoked hemodynamic responses *in vivo*. PLoS Biol 5:e119.

Zhang ZG, Zhang L, Ding G, Jiang Q, Zhang RL, Zhang X, Gan WB, Chopp M (2005) A model of mini-embolic stroke offers measurements of the neurovascular unit response in the living mouse. Stroke 36:2701–2704.

Zuo Y, Lin A, Chang P, Gan WB (2005a) Development of long-term dendritic spine stability in diverse regions of cerebral cortex. Neuron 46:181–189.

Zuo Y, Yang G, Kwon E, Gan WB (2005b) Long-term sensory deprivation prevents dendritic spine loss in primary somatosensory cortex. Nature 436:261–265.

NOTES